International Science and Technology Journal
المجلة الدولية للعلوم والتقنية
Volume 32 العدد
Aprilr 2023 ابريل
المجلة الدولية للعلوم والتقنية
ISTJ

Stress Singularity and Mesh Density of Finite Element Models under Combined Bending and Torsion Loading

Tariq R. Aboalhol

The Libyan Higher Technical Center for Training and Production

taboalhol@gmail.com

الملخص

أدى التقدم السريع في الكفاءة للمحاكاة الحاسوبية على مدى الثلاثين عامًا الماضية إلى جعل تحليل العناصر المحددة (FEAالأداة الرائدة في الصناعة للتنبؤ بالعمر التشغيلي للمنتج. ومع ذلك، فإن بعض التصاميم ذات اشكال هندسية معنية تحت احمال مختلفة حتى وان كانت صغيرة؛ غالبًا ما يتسبب في زيادة كبيرة وغير واقعية في توقع الإجهاد المراد دراسته. في هذه الدراسة، تم فحص نماذج في ثلاثة ابعاد بمستويات مختلفة من تحسين دقة الشبكة التحليلية (meshing) لقطعة دائرية مصمتة من الألومنيوم مثبتة بزاوية قائمة على حائط، معرضة لحمل الثني والتواء في نفس الوقت. نتائج الإجهاد مقارنة بالنموذج التحليلي وأظهرت تقاربًا جيدًا للشبكة من خلال زيادة دقة التنبؤ بالإجهاد في النموذج ذو الزاوية القائمة المدعومة بتقوس داخلي (fillet) بينما نموذج الزاوية القائمة العادية لم يظهر أي اقتراب (convergence) لقيم الإجهادات الحقيقة برغم من زيادة عناصر الشبكة التحليلية. يبدو أن الإجهاد الاقصى يصل الى قيم عالية جدا كلما زاد عدد عناصر الشبكة بسبب الإجهادات الأحادية (stress singularities).

الكلمات الرئيسية: تحليل العناصر المحدودة ، تحسين الشبكة ، تفرد الإجهاد.

Abstract

The rapid advance in computational efficiency over the last 30 years has made the finite element analysis (FEA) the industry-leading tool to predict a product's operational lifetime. Nevertheless, local design features under applied loading, even small loads; often cause a significant and unrealistic increase in local stress. 3-D FEA models with different levels of mesh

refinement of a right-angled aluminum bracket rod, with and without fillet profile, subjected to bending and torsion loadings were examined. Stress results compared with analytical model and showed a good mesh convergence through increasing resolution of the hexahedral elements in filleted corner case. The right angle model exhibited no convergence. As the number of elements increases to infinity, the peak stress appeared to go to infinity due to stress singularity.

Keywords: finite element analysis, mesh refinement, stress singularity.

1. Introduction

The finite element analysis is a powerful and prevalent numerical technique used mostly by engineers and scientists for obtaining approximate solutions to a variety of engineering problems (Huebner et al., 2008). FEA can predict how a product responds to real-life loading conditions, heat transfer, and fluid dynamic, among others (Lewis et al., 2004). It has improved over the decades to be more efficient, reliable and user friendly to confirm whether a product will break, wear out or function the way it was designed. Besides the FEA ability to evaluate the change in complex geometries with less time and resources as opposed to experimental tests, it makes it possible to perform numerous analyses of the same model under different situations or conditions (Fadiji et al., 2018).

There are several free or commercial FEA packages are now available for engineers and students. Generally, FEA software often features slick 3D pre- and post-processors for displaying the findings and viewing the model. While many FEA program packages have worked diligently to create cutting-edge software that is precise, understandable, and simple to use, the majority of users are not doing their part by mastering the engineering concepts and discipline needed to utilize these products properly (Plevris & Markeset, 2018). Even with highly sophisticated FEA simulations, the results are approximation to the actual solutions and consequently the user is accountable for ensuring that outputs are reliable and accurate. The concept of linear FEA is simple, but the

computations to achieve it are not. It is very easy to get FEA results that appear reasonable, but can be completely inaccurate if the user does not understand the method properly (Cook, 2007; Hughes, 2012; Zienkiewicz et al., 2005).

In FEA modelling and simulation, the user tries to determine the distribution of some field variable, for example, the stresses in structural mechanics analysis, the heat flux in thermal analysis, the flow rate in fluid dynamic analysis, and so forth. In general, the goal is to approximate a solution to a problem that is often challenging to solve analytically (Liu & Quek, 2013). The process starts with first dividing the problem domain into discrete elements (the mesh), often of simple geometry. The main variable in FEA is displacement, which is modeled by a linear combination of the Lagrange interpolation functions of the element. Then, strains and stresses can be determined once the nodes' displacement has been computed, for instance, by $\varepsilon = du/dx$ and $\sigma = E\,\varepsilon$. At the borders of the elements, the Lagrange functions are continuous, but their derivatives are not. Thus, the contour plot of displacements will seem continuous (no averaging is required), whereas the contour plot of stresses and strains will appear discontinuous. The degree of discontinuity may be lessened, if necessary, through mesh refinement. However, there are times where results of will define model inputs mislead users into blind acceptance of results in fancy graphics produced by powerful computers.

The scientific community has highlighted a number of issues, including the precision of contact surface stresses. (Coorevits et al., 2000; Crisfield, 2000; El-Abbasi & Bathe, 2001; Yue & Wahab, 2014), the ability to provide realistic prediction results within a reasonable computational time (Li et al., 2021; Papadakis et al., 2014), and stress singularities problem that have not been discussed in depth enough in any of the Finite Element textbooks and research (Bhavikatti, 2005; Cook, 2007; Coorevits et al., 2000; Fadiji et al., 2018; Gokhale et al., 2008; Huebner et al., 2008; Hughes, 2012; Lewis et al., 2004; Liu & Quek, 2013; Zienkiewicz et al., 2005).

Stress concentration and stress singularity are very essential feature in most mechanical component simulations. It can be located

in a structure where the stress is significantly greater than the surrounding region due to geometric discontinuities in the component (Norton, 2010). There has been a great amount of time and cost inherent in experimental data that formed a number of equations and methods to represent stress concentration factors to predict stresses and strains values in a few standard geometries available in several machine design handbooks (Sadegh & Worek, 2018; Shigley et al., 2004). The finite element analysis has been widely used as a complementary tool to study the stress concentration phenomena. To avoid unrealistic local stress peaks, many studies tackle the issue by carrying out convergence and mesh independence study to capture the system behavior with reasonable computation time (Boz et al., 2014; Dennis et al., 2005; Jung et al., 2020; Patil & Jeyakarthikeyan, 2018).

Generally, it is perceived that the mesh quality plays a great role on minimizing computational errors in FEA results. This broad concept has motivated the study behind the present work, which practically assesses mesh refinement of a re-entrant corner and peak stresses. The current study is to examine and compare FEA results of a right-angled aluminum bracket-rod model, which subjected to bending and torsion loadings with the same model that replaces a sharp right-angled feature with a fillet. Both FEA models' solutions are compared with the exact analytical solution.

2. Method

The model considered in the current study is a 2024-T4 aluminum bracket-rod with the dimensions shown in Fig.1. The rod is 1.5 inches in diameter and 6 inches long. The 1000 lbf applied at the tip of the arm, which connected to the free end of the rod. The other end of the rod fully bonded to a rigid wall. The rod, as a cantilever beam, is loaded in both bending and in torsion. The study assumes that largest bending stress will be in the top outer fiber at point A, while maximum torsional shear stress is expected uniformly distributed at the outer surface of the rod-wall fixed joint (Norton, 2010; Shigley, 2011).

2.1 The Analytical Solution

First, the deflection caused by combined loading is calculated then the stresses at point A as shown in Fig. 1. It is assumed that the wall and the arm are rigid bodies (i.e., there is no deformation in both). Axial deflection due to bending and rod twisting due to the torque contribute to the total deflection at the tip of the arm, where the force is applied. The material data sheet of Aluminum 2024-T4 are taken from the literature (Bauccio, 1993).

$$\delta_{total} = \delta_{\theta} + \delta_{bending} = 0.1991 + 0.0279 = 0.227\ in$$

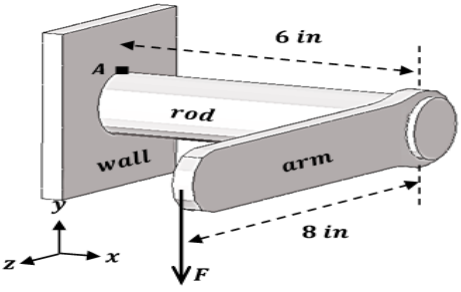

Fig. 1. The rod is under bending moment and torsion

The rod is loaded in both bending and in torsion. In Fig. 1 and Fig. 2, point A will have the highest stresses. The largest torsional shear stress is all around the outer circumference of the rod end that attached to the wall. The calculated stresses are given in Table 1.

Table 1. The theoretical values of the stresses (psi)

Axial stress component in x-direction (σ_x)	Maximum shear stress (τ_{max})	von Mises stress (σ')	Maximum principal stress (σ_1)
18108.3	15090.2	27660.9	24144.4

The following are the mathematical formulae that are used in the analytical solutions (Norton, 2010; Shigley, 2011).

Axial stress component in x-direction: there are no axial tensile stress nor compression along *x-axis*. There are bending (σ_x) and

shear stress (τ_{xz}) as showing in Fig. 2 and the governing equations (1) and (2).

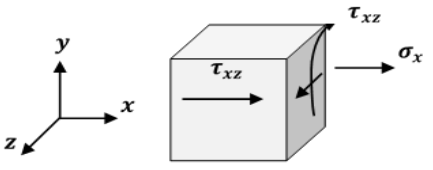

Fig. 2 Stress elements at point A within cross section of rod.

$$\sigma_x = \frac{Mc}{I} \quad (1)$$

$$\tau_{xz} = \frac{Tr}{J} \quad (2)$$

Maximum shear stress (τ_{max}) is given in Equation (3):

$$\tau_{max} = \sqrt{\frac{(\sigma_x - \sigma_z)^2}{2} + \tau_{xz}^2} \quad (3)$$

The maximum principal stress is given by (σ_1) in Equation (4):

$$\sigma_1 = \frac{(\sigma_x + \sigma_z)}{2} + \tau_{max} \quad (4)$$

The von Mises stress is given by (σ') in Equation (5):

$$\sigma' = \sqrt{\frac{((\sigma_x - \sigma_y)^2 + (\sigma_y - \sigma_z)^2 + (\sigma_z - \sigma_x)^2 + 6(\tau_{xy}^2 + \tau_{yz}^2 + \tau_{zx}^2))}{2}} \quad (5)$$

where, M is bending moment, c is rod's radius, I is the moment of inertia, T is the apple torque at the end of the arm, r is the radius of the rod's cross section and J is the polar moment of inertia for the shear.

2.2 Finite Element Analysis Model

A series of 3-dimension finite element models are generated for the assembly using reduced-integration eight-node hexahedral elements. The best way for assessing mesh quality is to refine it until important results; for example, maximum von Mises stress in a defined site does not change significantly with subsequent refinements.

2.3 Element Quality

The Mesh Metric tool in ANSYS Workbench is used to detect poor quality elements, which may potentially contribute to solution errors. Because the rod's shape has a perfect cylindrical geometry, all generated meshes are excellent based criteria shown in Table 2.

Table 2. Mean and standard deviation of models' elements metric

Mesh Metric	Average	Standard deviation	Quality	
			Worst	Perfect
Aspect ratio	1.20	0.13	>3.0	1.0
Jacobian ratio	0.93	0.06	-1.0	1.0
Skewness	0.07	0.008	1.0	0.0

The Aspect Ratio measures the quality of the elements; a perfect element has an aspect ratio of 1, whereas elements with greater ratios than 3 have poorer shapes. For example, a perfect cube has equal and square-shaped sides. Jacobian ratio is a measurement of how far an element is from having the optimal shape. The jacobian value goes from -1.0 to 1.0, with 1.0 representing an element with the ideal shape. Skewness is the angle at which an element's quality is measured in relation to the angles of ideal element types. In hexahedral element, the perfect right angle in each corner.

2.4 Mesh Refinement

Mesh refinement method in this study is based on the number of elements on circular face in one of the rod end. In a rigorous refinement process that starts with a coarse mesh using average edge length of 0.3 in (7.6 mm) to ultra-fine mesh with 0.057 in (1.45 mm), which generates 34 models. This is proposed to study whether the element provides a greater level of accuracy to stress results. In Fig. 3 below is a set of images display the variation of grid resolution. Note that the 34 right angle models and 34 fillet models have the exact same number of nodes and elements. Finite element software package, ANSYS Workbench, is employed to construct 34 models with various mesh sizes for the same geometry.

2.5 Rod with Right-Angled Shape

Setting up a FEA model that has various parts creating an assembly with well-defined material properties, realistic boundary and loading conditions, and running the model is one-step. Making

sense and interpreting the results can be, in some structures, a very important and challenging step.

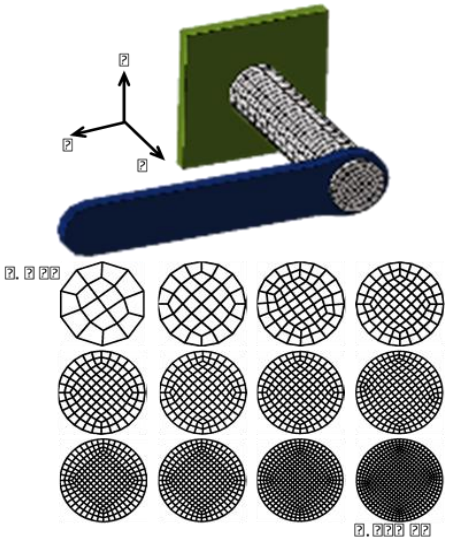

Fig. 3 Sample of model mesh refinements

Therefore, the current study takes a simple and straightforward approach to computationally investigate two sets of FEA subjected to same combined loading conditions. The first model with right-angled shape between the rod and the wall, while the second has a fillet replaces sharp re-entrant corner. Moreover, to avoid inconsistency that may disturb mesh convergence when the two models are compared, the numbers of nodes and element are kept the same. However, a small set of rod elements are morphed to create a 0.6-inch fillet as illustrated in Fig.4.

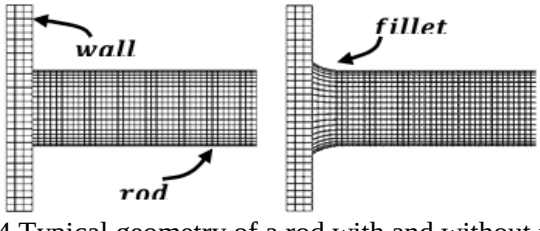

Fig. 4 Typical geometry of a rod with and without fillet.

3.Results and Discussions

Three-dimensional finite element models with 34 different mesh densities are used to analyze the stresses for bracket rod with sharp right angle corner at first using static analysis. Then, the same mesh family is generated with the exact mesh densities in another set that has sharp corner morphed into a fillet in each model with no changes in the number of nodes and elements as shown in Fig. 4. The results are post-processed to generate normal bending stresses, the equivalent (von Mises) stresses, maximum shear stress, maximum principal stresses and total deformation. A plot of the stresses versus the mesh refinements for all models is shown in Fig. 5 and results of selected models are summarized in Table 3.

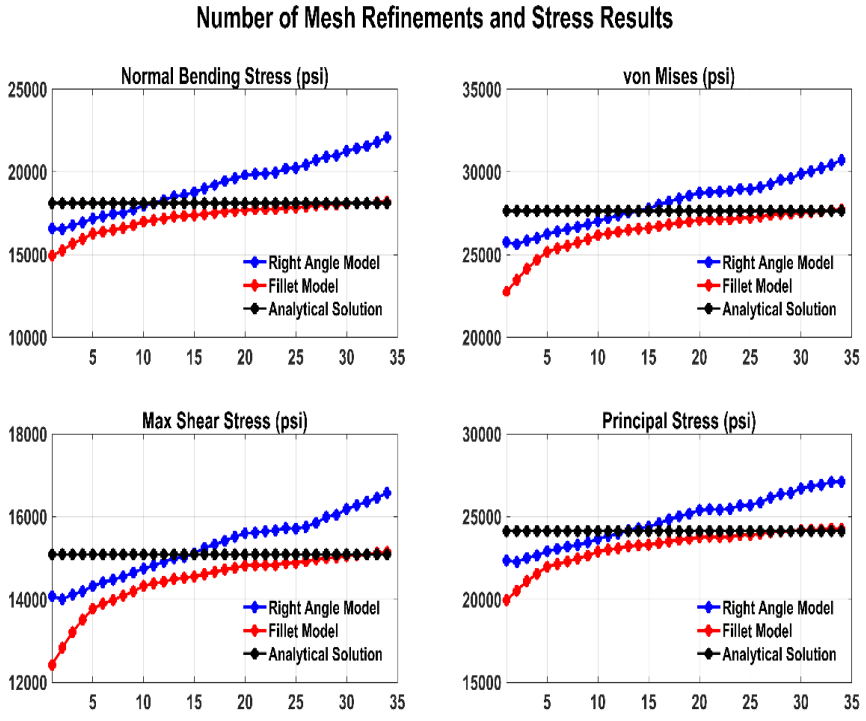

Fig. 5. Stresses vs. mesh density in right-angled and filleted models where the vertical axis in each chart represents the stress (psi) and the horizontal axis shows the model number.

Table 3. Number of elements used in each of FEA models vs. peak stresses

Model	No. of Elements	**Normal Bending Stress**		Analytical (psi)	18108.296
		Right Angle		Fillet	
		Magnitude(psi)	Change(%)	Magnitude(psi)	Change(%)
1	208	16578.6	8.4	14940.3	17.5
10	2688	17967.2	0.8	16995.9	6.1
20	10800	19795.6	9.3	17715.1	2.2
30	33088	21268.8	17.5	18085.3	0.1
34	60480	22095.8	22.0	18110.5	0.0

Model	No. of Elements	**Max Shear Stress**		Analytical (psi)	15090.246
		Right Angle		Fillet	
		Magnitude(psi)	Change(%)	Magnitude(psi)	Change(%)
1	208	14082.2	6.7	12420.8	17.7
10	2688	14747.5	2.3	14331.1	5.0
20	10800	15602.7	3.4	14820.7	1.8
30	33088	16186.0	7.3	15052.1	0.3
34	60480	16579.1	9.9	15110.9	0.1

Model	No. of Elements	**von Mise Stress**		Analytical (psi)	27660.879
		Right Angle		Fillet	
		Magnitude(psi)	Change(%)	Magnitude(psi)	Change(%)
1	208	25761.1	6.9	22750.4	17.8
10	2688	27041.8	2.2	26183.7	5.3
20	10800	28738.7	3.9	27107.3	2.0
30	33088	29899.0	8.1	27545.4	0.4
34	60480	30733.9	11.1	27717.8	0.2

Model	No. of Elements	**Max Principal Stress**		Analytical (psi)	24144.394
		Right Angle		Fillet	
		Magnitude(psi)	Change(%)	Magnitude(psi)	Change(%)
1	208	22371.5	7.3	19969.5	17.3
10	2688	23666.4	2.0	22895.9	5.2
20	10800	25393.7	5.2	23766.9	1.6
30	33088	26709.3	10.6	24193.6	0.2
34	60480	27106.7	12.3	24175.4	0.1

It undoubtedly appears that the values of maximum stresses are completely dependent on the level of mesh density in the right-

angled bracket models. In this case, the peak stress values increase as the mesh density level increases and diverge from the analytical solutions. There is no convergence in sight because as the peak stresses at these sites approaching to infinity, the element size coming closer and closer to zero. On other hand, fillet model shows steady convergence across 4 types of stress results. Although, they all start far from the analytical solutions in course meshes, then the stress results gradually approach closer to the analytical results. The reason can be that the fillet feature smooths out the discontinuity between the rod and the wall that is seen in the right-angled model. Instead of sharp right-angle shape with stress concentrating at a small number of interface elements between the wall and the rod, the shape of the fillet allows more elements residing on a larger area to share the load and consequently reasonable peak stress values near the analytical results.

In right-angled models, the higher bending stress contour pattern shrinks and clearly confines to a small space at the sharp corner as the mesh density increases as shown in Fig. 6.

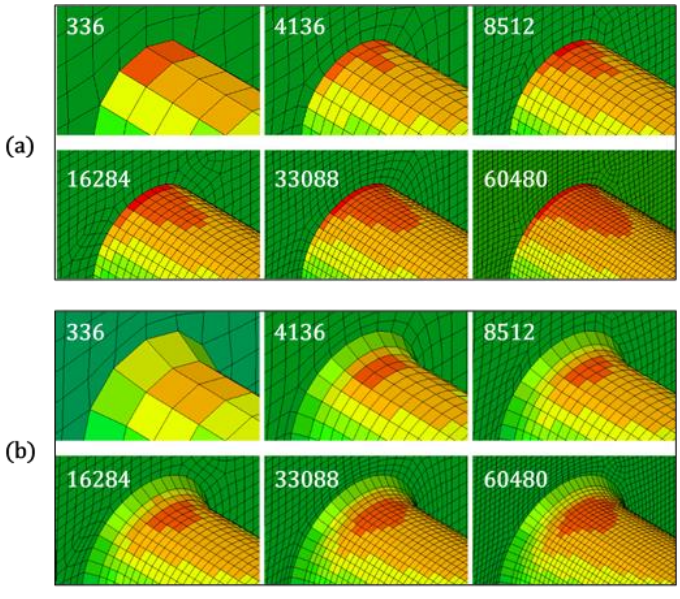

Fig. 6. Peak bending stresses vs. mesh density in (a) right-angled (b) filleted models

This phenomenon unobserved in filleted models. FEA calculates stress in the Gaussian points of an element after interpolating nodes translations. To get a single stress value at a node, the estimated stress value is averaged over the contributing elements. Typically, where force is exerted or transferred, a high stress develops and gradually decreases as moving away from the location where load is being transferred. It is worth mentioning that peak stress results are useless around the sharp re-entrant edges. This is the region of most engineering interest in the bracket.

Stress results show that mesh density affects the precision of FE calculations significantly. High local stress gradients may go undetected in coarser meshes because nodes are spaced farther apart from the load application location. The unaveraged stress contour plot can be used to accurately locate where failure initiates and reconsider design alternatives in complex geometries or discontinuities as in Fig. 7.

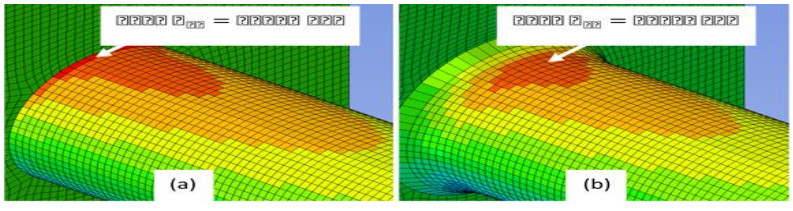

Fig. 7. Unaveraged stress contour plots: (a) right-angled (b) filleted model

The fillets efficiently boost the load bearing capacity of components by distributing the stress across a larger region. In general, a sharp corner will always have a modest fillet radius in the actual world. Therefore, tiny fillets to sharp corners to depict a more accurate real-world model must be included because this detail is not built into the FEA model.

4. Conclusion

Because FEA software is becoming more widely available, there is a risk that uninformed users will depend on its predictions without having the specialized knowledge necessary to properly setup up simulation models or identify any potential calculation

inaccuracies. A mesh refinement and a more potent computer are sometimes believed to be the solutions to all FEA accuracy issues, however this is another oversimplification that is untrue in practice. The user can easily be betrayed into accepting the program's generated results without question. In stress analysis, failing to appropriately treat local geometry discontinuities can contribute to calculation errors. It is essential to new FEA users and engineers detect them and use alternatives (a fillet for re-entrant corner, for example) to avoid unrealistic predictions. A quick method to examine probable singularity locations in the mesh is to perform a mesh sensitivity analysis. Finally, stress singularities do not always indicate that other parts of the FEA model's stress findings are inaccurate. Only the nodes closest to the singularity will be affected by the singularity's impact on stress.

5. Acknowledgments

This study was supported by Libyan Academy for Postgraduate Studies. The author thanks Dr. Khaled Abdusamad, the head of Mechanical Engineering Department at School of Applied Science and Engineering, for Simulation Lab assistance.

6. References

Bauccio, M. (1993). *ASM metals reference book*. ASM international.

Bhavikatti, S. (2005). *Finite element analysis*. New Age International.

Boz, Z., Erdogdu, F., & Tutar, M. (2014). Effects of mesh refinement, time step size and numerical scheme on the computational modeling of temperature evolution during natural-convection heating. *Journal of Food Engineering, 123*, 8-16.

Cook, R. D. (2007). *Concepts and applications of finite element analysis*. John wiley & sons.

Coorevits, P., Hild, P., & Pelle, J.-P. (2000). A posteriori error estimation for unilateral contact with matching and non-matching meshes. *Computer Methods in Applied Mechanics and Engineering, 186*(1), 65-83.

Crisfield, M. (2000). Re-visiting the contact patch test. *International Journal for Numerical Methods in Engineering, 48*(3), 435-449.

Dennis, J., Fournier, A., Spotz, W. F., St-Cyr, A., Taylor, M. A., Thomas, S. J., & Tufo, H. (2005). High-resolution mesh convergence properties and parallel efficiency of a spectral element atmospheric dynamical core. *The International Journal of High Performance Computing Applications, 19*(3), 225-235.

El-Abbasi, N., & Bathe, K.-J. (2001). Stability and patch test performance of contact discretizations and a new solution algorithm. *Computers & Structures, 79*(16), 1473-1486.

Fadiji, T., Coetzee, C. J., Berry, T. M., Ambaw, A., & Opara, U. L. (2018). The efficacy of finite element analysis (FEA) as a design tool for food packaging: A review. *Biosystems Engineering, 174*, 20-40.

Gokhale, N. S., Deshpande, S. S., Bedekar, S. V., & Thite, A. (2008). *Practical Finite Element Analysis, Finite to Infinite*. Pune.

Huebner, K. H., Dewhirst, D. L., Smith, D. E., & Byrom, T. G. (2008). *The finite element method for engineers*. John Wiley & Sons.

Hughes, T. J. (2012). *The finite element method: linear static and dynamic finite element analysis*. Courier Corporation.

Jung, D., Lee, D., Kim, M., Kim, H., & Park, S.-K. (2020). Mesh convergence test system in integrated platform environment for finite element analysis. *The Journal of Supercomputing, 76*, 5244-5258.

Lewis, R. W., Nithiarasu, P., & Seetharamu, K. N. (2004). *Fundamentals of the finite element method for heat and fluid flow*. John Wiley & Sons.

Li, G., Liu, M., & Zhao, S. (2021). Reduced computational time in 3D finite element simulation of high speed milling of 6061-T6 aluminum alloy. *Machining Science and Technology, 25*(4), 558-584.

Liu, G.-R., & Quek, S. S. (2013). *The finite element method: a practical course*. Butterworth-Heinemann.

Norton, R. L. (2010). *Machine design*. Prentice Hall.

Papadakis, L., Loizou, A., Risse, J., Bremen, S., & Schrage, J. (2014). A computational reduction model for appraising structural effects in selective laser melting manufacturing: a methodical model reduction proposed for time-efficient finite element analysis of larger components in Selective Laser Melting. *Virtual and Physical Prototyping*, *9*(1), 17-25.

Patil, H., & Jeyakarthikeyan, P. (2018). Mesh convergence study and estimation of discretization error of hub in clutch disc with integration of ANSYS. IOP Conference Series: Materials Science and Engineering,

Plevris, V., & Markeset, G. (2018). Educational Challenges in Computer-based Finite Element Analysis and Design of Structures.

Sadegh, A. M., & Worek, W. M. (2018). *Marks' Standard Handbook for Mechanical Engineers*. McGraw-Hill Education.

Shigley, J. (2011). *Shigley's mechanical engineering design. 2011*. Tata McGraw-Hill Education.

Shigley, J. E., Mischke, C. R., & Brown Jr, T. H. (2004). *Standard handbo*

Yue, T., & Wahab, M. A. (2014). Finite element analysis of stress singularity in partial slip and gross sliding regimes in fretting wear. *Wear*, *321*, 53-63.

Zienkiewicz, O. C., Taylor, R. L., & Zhu, J. Z. (2005). *The finite element method: its basis and fundamentals*. Elsevier.